FEATURE ARTICLE

Glassiness of Thermotropic Liquid Crystals across the Isotropic−Nematic Transition

Dwaipayan Chakrabarti*,†,‡ and Biman Bagchi*,†

Solid State and Structural Chemistry Unit, Indian Institute of Science, Bangalore 560 012, India, and Department of Chemistry, University of Cambridge, Cambridge CB2 1EW, United Kingdom

Received: April 3, 2007; In Final Form: July 16, 2007

The orientational dynamics of thermotropic liquid crystals across the isotropic−nematic phase transition have traditionally been investigated at long times or low frequencies using frequency domain measurements. The situation has now changed significantly with the recent report of a series of interesting transient optical Kerr effect (OKE) experiments that probed orientational relaxation of a number of calamitic liquid crystals (which consist of rod-like molecules) directly in the time domain, over a wide time window ranging from subpicoseconds to tens of microseconds. The most intriguing revelation is that the decay of the OKE signal at short to intermediate times (from a few tens of picoseconds to several hundred nanoseconds) follows multiple temporal power laws. Another remarkable feature that has emerged from these OKE measurements is the similarity in the orientational relaxation behavior between the isotropic phase of calamitic liquid crystals near the isotropic−nematic transition and supercooled molecular liquids, notwithstanding their largely different macroscopic states. In this article, we present an overview of the understanding that has emerged from recent computational and theoretical studies of calamitic liquid crystals across the isotropic−nematic transition. Topics discussed include (a) single-particle as well as collective orientational dynamics at a short-to-intermediate time window, (b) heterogeneous dynamics in orientational degrees of freedom diagnosed by a non-Gaussian parameter, (c) fragility, and (d) temperature-dependent exploration of underlying energy landscapes as calamitic liquid crystals settle into increasingly ordered mesophases upon cooling from the high-temperature isotropic phase. A comparison of our results with those of supercooled molecular liquids reveals an array of analogous features in these two important classes of soft matter systems. We further find that the onset of growth of the orientational order in the parent nematic phase induces translational order, resulting in *smectic-like layers in the potential energy minima of calamitic systems* if the parent nematic phase is sandwiched between the high-temperature isotropic phase and the low-temperature smectic phase. We discuss implications of this startling observation. We also discuss recent results on the orientational dynamics of discotic liquid crystals that are found to be rather similar to those of calamitic liquid crystals.

I. Introduction

Soft condensed matter is ubiquitous in nature. It encompasses diverse physical systems, isotropic liquids with short-range order on the one hand and liquid crystals with long-range order in their anisotropic mesophases on the other. The concepts of broken symmetry and order parameter have emerged as useful tools for a unified description of this rich diversity.[1] Anisotropy in molecular shape plays a crucial role in the exotic phase behavior that thermotropic liquid crystals exhibit upon temperature variation.[2,3] Calamitic liquid crystals consist of rodlike molecules; discotic liquid crystals comprise disclike molecules. For both calamitic and discotic liquid crystals, the high-temperature phase is the isotropic with no long-range order. Upon cooling, various mesophases appear differing in order and symmetry. The simplest of the ordered phases is the nematic, which has a long-range orientational order but no long-range translational order. The transition to the nematic phase from the isotropic phase is known to be weakly first order in nature with some characteristics of continuous transitions.[4] Although both calamitic and discotic liquid crystals exhibit the nematic phase, the onset of translational order upon lowering the temperature further results in different mesophases. For calamitic liquid crystals, one typically observes a smectic phase, which is characterized by the appearance of partial translational order in layers in addition to a further increase in orientational order.[2,3] In the case of discotic liquid crystals, the columnar phase results from stacking of mesogens on top of each other, giving rise to a columnar structure.

The orientational dynamics in the isotropic phase of liquid crystals near the isotropic−nematic (I−N) transition have drawn much attention over the years.[5−15] The focus has often been on the verification of the Landau−de Gennes (LdG) theory, which predicts a long-time exponential decay with a strongly temperature-dependent time constant.[5−7,9,10] However, a series of recent optical heterodyne-detected optical Kerr effect (OHD-OKE) measurements by Fayer and co-workers revealed a rather complex relaxation pattern with rich short-time dynamics in the isotropic phase of a number of calamitic liquid crystals near

* E-mails: bbagchi@sscu.iisc.ernet.in; dc430@cam.ac.uk.
† Indian Institute of Science.
‡ University of Cambridge.

10.1021/jp079516w CCC: $37.00
Published on Web 09/20/2007

Dwaipayan Chakrabarti did his undergraduate in the Presidency College under the University of Calcutta in India and went on to complete his postgraduate study in Chemistry at the same university. He obtained his Ph.D. in 2006 from the Indian Institute of Science, Bangalore under the supervision of Professor Biman Bagchi. He is currently a Marie Curie Incoming International Research Fellow in the Department of Chemistry at the University of Cambridge, working with Dr. David J. Wales. His research employs computer simulation techniques to explore structure, thermodynamics, and dynamics of soft matter systems, often in connection with their underlying energy landscapes.

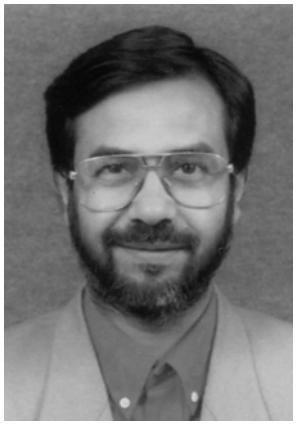

Biman Bagchi (born 1954) received his undergraduate degree from the Presidency College, Calcutta University (W. Bengal, India), in 1976. He obtained his Ph.D. degree from Brown University (Providence, RI) in 1980, with Professor Julian H. Gibbs as his advisor. He was a Research Associate at the James Franck Institute, University of Chicago (1981−1983), where he worked with Professors David W. Oxtoby, Graham Fleming, and Stuart Rice, and the University of Maryland (with Robert Zwanzig) before returning to India in the fall of 1984 to join the faculty of the Indian Institute of Science, Bangalore. He is currently the Amrut Mody Chair Professor of Chemical Sciences and is a Fellow of the Indian Academy of Sciences and also of the Third World Academy, Trieste. His research interests include chemical reaction dynamics, molecular relaxation and transport processes in liquids and electrolyte solutions, phase transition and nucleation phenomena, protein and DNA hydration dynamics, supercooled liquids, liquid crystals, micelles, and polymers.

the I−N transition.[12−14] On the basis of OHD-OKE measurements with four calamitic liquid crystals in the isotropic phase and five supercooled molecular liquids, a comparison of their orientational dynamics was drawn.[16] The most striking feature that emerged from this comparison is an identical description of the time-dependent OHD-OKE data for all nine liquids. The description involves a power law at short times and an exponential decay at long times, with a second power law in the crossover region.[16]

A liquid enters the supercooled regime below its freezing temperature T_m upon cooling sufficiently fast to circumvent crystallization. The regime has a lower bound at the glass transition temperature, T_g. At T_g, which usually occurs around $2T_m/3$,[17,18] the metastable liquid transforms to an amorphous solid, called glass, that lacks long-range spatial order. Several features of slow dynamics of supercooled liquids continue to pose challenges to experimental, theoretical, and computational research alike.[17,18] However, the existing evidence seems to have ruled out the involvement of a true phase transition at T_g;[18] now there appears a consensus that the laboratory glass transition is a kinetic phenomenon caused by a dramatic slowdown of molecular motion. Given the contrasting scenario in regard to the involvement of a thermodynamic phase transition, the similarity in orientational dynamics between the isotropic phase of calamitic liquid crystals near the I−N transition and supercooled liquids is, indeed, appealing.

Computer simulations have proven an indispensable tool to understand properties of soft matter and link theoretical models to experiments, often with an insight into the microscopic level.[19] Here, we provide an overview of our recent computational approach to investigate complex dynamics in thermotropic liquid crystals and supercooled molecular liquids in pursuit of analogous features. The emphasis is on the short-to-intermediate time window, which revealed intriguing dynamics in recent experiments. In the next section, we summarize the experimental results that set up the background of our computational approach. Section III presents a summary of the existing theoretical attempts to interpret such complex dynamical features. We next briefly describe the model systems undertaken in our computational studies before summarizing our results on analogous dynamics in Section V. At a fundamental level, the potential energy surface of a system is known to govern its structure, thermodynamics, and dynamics. In particular, a computational approach that explores how a system samples its underlying potential energy surface has provided a wealth of information about complex dynamics in supercooled liquids.[20−24] The success of such an approach led us to investigation of the energy landscapes of calamitic liquid crystals, which is revisited in Section VI as an essential part of our quest to explore the analogy between these two important classes of soft matter systems. Section VII presents a structural analysis of the potential energy minima, which has important implication on the interplay between the orientational and translational order in calamitic mesophases. Section VIII concludes with a discussion.

II. Background: Experimental Results

Recent OHD-OKE measurements by Fayer and co-workers have generated renewed interests in the orientational dynamics across the I−N transition.[12−14] For times greater than ∼1 ps, the OKE signal is the negative time derivative of the correlation function of the linear susceptibility at zero wave vector.[12,25] In this time domain, the linear susceptibility may be considered as the sum of molecular polarizability tensors for a liquid composed of rigid molecules. These OKE experiments thus probe the collective orientational dynamics. For the measurements in the isotropic phase with a number of calamitic liquid crystals for which the molecular aspect ratio varies between 3.26 and 4.56, the OHD-OKE signal was probed over a time window spanning from subpicoseconds to tens of nanoseconds. The OKE signal was found to decay exponentially only at long times beyond several nanoseconds with a strongly temperature-dependent time constant. The most notable feature of these measurements, however, concerns a short-to-intermediate time window in which two power law decay regimes were observed.

The exponent of the power law, which was observed before the crossover regime, appeared to be temperature-independent and was found to be in the range between 0.63 and 0.76 for the systems studied.

In more recent OHD-OKE measurements, a number of homeotropically aligned nematic liquid crystals were studied over more than 6 decades of time (from 500 fs to a few tens of microseconds).[26,27] The OKE signal was found to follow a rather temperature-independent power law decay at long times spanning over more than 2 decades. On shorter time scales (from ~3 ps to ~1 ns), in contrast, a temperature-dependent power law was observed. The exponent of the temperature-dependent power law, called the intermediate power law to distinguish it from the final power law that was observed at long times, was found to vary linearly with the orientational order parameter.[26,27]

In another series of OHD-OKE experiments with five molecular liquids (for which the aspect ratio varied between 1.5 and 2.11) in the supercooled regime, a relaxation pattern similar to that of the isotropic phase of calamitic liquid crystals was observed.[28,29] The "intermediate" power law decay with temperature-independent exponents close to -1 was observed from ~2 ps to 1−10 ns for all five liquids over a wide range of temperatures from well above the mode-coupling theory (MCT) critical temperature, T_c, to close to it. Such an exponent value for the decay of the negative time derivative of a correlator translates into a nearly logarithmic decay of the correlator itself.[28,29] The intermediate power law decay was followed by a second power law decay at a longer time scale and the final exponential decay.

The correspondence of these time domain OHD-OKE experiments with frequency domain measurements is worth noting. When expressed in terms of frequency dependence, the intermediate power law in the time domain (corresponding to nearly logarithmic decay of the correlator) translates into a very weak frequency dependence of the imaginary part of the susceptibility, a phenomenon known as nearly constant loss (NCL).[29] This has been observed for a number of glass formers and ionic conductors.[30−32] In particular, the depolarized light-scattering data of polyisobutylene suggested the existence of NCL over a rather broad frequency range extending beyond 10 GHz across the glass transition temperature.[31]

III. Theoretical Analysis

Several attempts have been undertaken to put forward an explanation of the power law decay observed in these two soft matter systems at short-to-intermediate time scales. Within the framework of MCT, the power law decay in supercooled liquids is generally attributed to the nonlinear coupling between the memory function and the dynamic structure factor.[33] Götze and Sperl showed that a schematic model, which incorporated translation-rotation coupling within MCT, could explain the nearly logarithmic decay as a manifestation of the β-peak phenomenon.[34] On the other hand, a schematic mode coupling theory that is based on the Sjörgen model with additional terms tailored specifically for mesogens in the isotropic phase could reproduce the OKE data for a number of liquid crystalline systems over approximately 6 decades of time.[35] However, an understanding of the physical nature of the mode, to which the orientational correlation function is coupled, is beyond the scope of such a schematic model. Alternatively, it was suggested that power law decay could result either from a power law growth of the memory kernel or from softening of the free energy surface in the vicinity of the I−N transition due to fluctuations in the orientational order parameter.[36] In an analytic model of structural relaxation in complex liquids, non-Markovian dynamics in a bistable potential under the action of fractional Gaussian noise was also found to capture some of the features of the experimental data, including the short-to-intermediate time power law day.[37]

The origin of the NCL, which has been suggested to be a universal phenomenon in glass-forming systems, even though it is masked by other relaxation contributions in many cases,[31] is also not well-understood at present. Although no rigorous theoretical explanation exists, the NCL is likely to originate from fluctuations when all the molecules are still caged.[32] Such a suggestion has received support from recent simulation of an ionic conductor.[38] Alternatively, the asymmetric double-well potential (ADWP) model[39] and anharmonic model[40] of fast relaxation were shown to capture the NCL under certain assumptions.[31]

IV. Model Systems

An integral part of the computational approach is molecular modeling, which is quite demanding in the case of liquid crystals because of their rich phase behavior.[41] Although atomistic models could, in principle, serve the purpose, molecular models in which mesogens are approximated with particles having well-defined anisotropic shape find their utility in obtaining a rather generalized view. A simple approach along this line involves consideration of purely repulsive models involving hard bodies.[42] This extreme choice is inspired by the idea that the equilibrium structure of a dense liquid is essentially determined by the repulsive forces that fix the molecular shape.[43] Such an approach is appealing for its simplicity.[42] However, temperature plays no direct role in purely repulsive models, unlike in thermotropic liquid crystals.

In studies of thermotropic liquid crystals within the purview of the present article, we thus undertook molecular dynamics simulation studies of model systems, in which mesogens, approximated with ellipsoids of revolution, interacted with the Gay−Berne (GB) pair potential or one of its variants.[44] The GB pair potential, in which each ellipsoid of revolution has a single-site representation, is an elegant generalization of the extensively used isotropic Lennard-Jones potential to incorporate anisotropy in both the attractive and repulsive parts of the interaction.[44] In the GB pair potential, the ith ellipsoid of revolution is represented by the position, $\mathbf{r}_i$, of its center of mass and a unit vector, $\hat{\mathbf{e}}_i$, along the long axis in the case of a prolate. The GB interaction between two ellipsoids of revolution i and j is given by

$$U_{ij}(\mathbf{r}_{ij}, \hat{\mathbf{e}}_i, \hat{\mathbf{e}}_j) = 4\epsilon(\hat{\mathbf{r}}_{ij}, \hat{\mathbf{e}}_i, \hat{\mathbf{e}}_j)(\rho_{ij}^{-12} - \rho_{ij}^{-6}) \qquad (1)$$

where $\rho_{ij} = (r_{ij} - \sigma(\hat{\mathbf{r}}_{ij}, \hat{\mathbf{e}}_i, \hat{\mathbf{e}}_j)/\sigma_{GB}$. Here σ_{GB} defines the cross-sectional diameter, $\mathbf{r}_{ij}$ is the separation between the center of mass of the molecules i and j, and $\hat{\mathbf{r}}_{ij} = \mathbf{r}_{ij}/r_{ij}$ is a unit vector along $\mathbf{r}_{ij}$. Both the molecular shape parameter, σ, and the energy parameter, ϵ, depend on the unit vectors $\hat{\mathbf{e}}_i$ and $\hat{\mathbf{e}}_j$ as well as on $\hat{\mathbf{r}}_{ij}$ The description of the potential can be found in detail elsewhere.[45,46] Note that unlike in refs 45 and 46, the GB potential parameters, which set up the length and energy scales, are denoted here by σ_{GB} and ϵ_{GB}, respectively. It is important to recognize that the GB pair potential defines a family of models, each member of which is characterized by a set of four parameters (κ, κ', μ, ν). Here $\kappa = \sigma_{ee}/\sigma_{ss}$ is the aspect ratio of the ellipsoid of revolution ($\kappa > 1$for a prolate and $\kappa < 1$ for an oblate), σ_{ee} being the molecular length along the principal symmetry axis, $\sigma_{ss} = \sigma_{GB}$, $\kappa' = \epsilon_{ss}/\epsilon_{ee}$, where ϵ_{ss} is the depth of

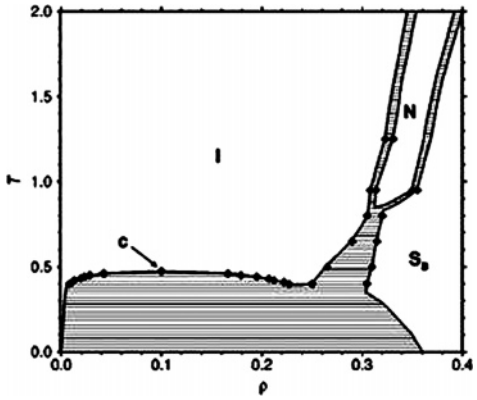

Figure 1. The phase diagram of the Gay−Berne model with the original and the most studied parametrization ($\kappa = 3$, $\kappa' = 5$, $\mu = 2$,$\nu = 1$) in the temperature-density plane as obtained from computer simulations. Filled diamonds mark simulation results; the phase boundaries away from these points are drawn as a guide only. The domains of the thermodynamic stability of the isotropic (I), nematic (N), and smectic (S_B) phases are shown. The liquid−vapor critical point is denoted by c. Two-phase regions are shaded. Reprinted with permission from ref 45. Copyright 1998 by the American Physical Society.

the minimum of the potential for a pair of ellipsoids of revolution aligned parallel in a side-by-side configuration and ϵ_{ee} is the corresponding depth for the end-to-end alignment, and μ and ν are two adjustable parameters. It follows that κ provides a measure of the shape anisotropy, which is essential for the existence of the mesophases, and a measure of the anisotropy in the well depth is provided by κ'. The well depth is also controlled by the other two parameters, μ and ν. Following the suggestion of Bates and Luckhurst,[47] each member of the family of GB models is represented by GB(κ, κ', μ, ν). The GB pair potential has been used extensively in studies of thermotropic liquid crystals with the original parametrization (3, 5, 2, 1) for which the global phase diagram is known.[46] In Figure 1, the global phase diagram of the GB(3, 5, 2, 1) model is shown on the temperature−density plane.[45] This would be instructive, since much of the work discussed here involved the study of the GB(3, 5, 2, 1) system as the temperature was varied along isochors. For one-component GB systems, all quantities are given here in reduced units, defined in terms of the GB potential parameters σ_{GB} and ϵ_{GB}, each of which was set to be unity: length in units of σ_{GB}; temperature in units of ϵ_{GB}/k_B, k_B being the Boltzmann constant; and time in units of $(\sigma_{GB}^2 m/\epsilon_{GB})^{1/2}$, m being the mass of the ellipsoids of revolution. The mass and the moment of inertia of the ellipsoids were set equal to unity.[45] Details of the method of simulations can be found elsewhere.[48]

In order to study a model system of supercooled liquids with orientational dynamics, we introduced a binary mixture.[48] The focus of molecular dynamics simulation studies on supercooled liquids has largely been on atomic systems involving only translational degrees of freedom (TDOF), even though most of the good glass-formers in reality are molecular systems.[49,50] The system we investigated is a 50:50 mixture of spheres and ellipsoids of revolution. The spheres interacted with each other via the Lennard-Jones pair potential, and the interaction between two ellipsoids of revolution was modeled by GB(2, 5, 2, 1). The interaction between a sphere and an ellipsoid of revolution (S−E) was given by the pair potential suggested by Cleaver and co-workers.[51,52] For the binary mixture, all quantities are given in reduced units, defined in terms of the Lennard-Jones potential parameters σ_{LJ} and ϵ_{LJ}. The various energy and length parameters of the interaction potentials for the binary mixture were chosen as follows: $\epsilon_{LJ} = 1.0$, $\epsilon_{GB} = 0.5$, $\epsilon_{SE} = 1.5$, $\sigma_{LJ} = 1.0$, $\sigma_{GB} = 1.0$, and $\sigma_{SE} = 1.0$. For the interaction between a sphere and an ellipsoid of revolution, the ratio ϵ_S/ϵ_E, which controls the configurational side-to-end well-depth anisotropy, was set equal to 5 and $\mu = 2$. The choice of ellipsoids of revolution as the component with orientational degrees of freedom (ODOF) in the binary mixture was motivated by our intention to adopt a comparative approach, given that ellipsoids of revolution serve well to comprise a standard anisotropic system in studies of thermotropic liquid crystals. The presence of spheres as the second component, a relatively small aspect ratio for the ellipsoids of revolution, and the chosen interaction parameters ensured that neither any phase separation occurred nor any liquid crystalline phase with orientational order appeared in the binary mixture, even at the lowest temperature studied at a high density within the length of our molecular dynamics simulations. The method of simulations has been described at length in ref 48.

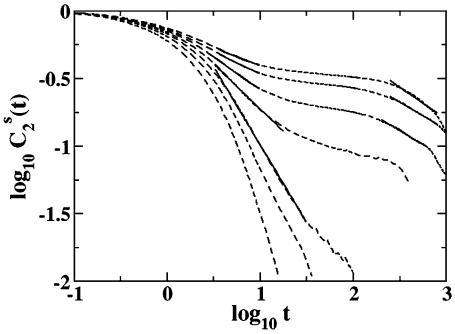

Figure 2. Time dependence of the single-particle second-rank orientational time correlation function in a log−log plot for a 500-particle model liquid crystalline system GB(3, 5, 2, 1) across the I−N transition at several temperatures at the isochor at density $\rho = 0.32$. From left to right, the temperature, T, falls gradually: $T = 2.008$, 1.697, 1.499, 1.396, 1.310, 1.199, and 1.102. The continuous lines are the linear fits to the data, showing the power law decay regimes (data from ref 48).

V. Results on Analogous Dynamics

1. Short-to-Intermediate Time Orientational Dynamics. We discuss here *both* the single-particle and collective orientational dynamics of a prototype model system of calamitic liquid crystals across the I−N transition. The I−N transition was marked by a jump in the average orientational order parameter $<P_2>$ as the temperature was varied along an isochor. The orientational order parameter $<P_2>$ was obtained as the largest eigenvalue of the ordering matrix $\mathbf{Q}$: $\mathbf{Q}_{\alpha\beta} = 1/N\sum_{i=1}^{N} 1/2\,(3e_{i\alpha}e_{i\beta} - \delta_{\alpha\beta})$, where $e_{i\alpha}$ is the α component of the unit orientational vector, $\hat{\mathbf{e}}_i$, in the space-fixed frame, and N is the number of particles in the system.[53] In Figure 2, we show the time evolution of the single-particle, second-rank orientational time correlation function (OTCF) at several temperatures in a log−log plot. The single-particle lth rank OTCF is defined by

$$C_l^s(t) = \frac{<\sum_i P_l(\hat{\mathbf{e}}_i(t)\cdot\hat{\mathbf{e}}_i(0))>}{<\sum_i P_l(\hat{\mathbf{e}}_i(0)\cdot\hat{\mathbf{e}}_i(0))>} \qquad (2)$$

where P_l is the lth rank Legendre polynomial, and the angular brackets denote ensemble averaging. $C_2^s(t)$ is directly accessible in experiments. For example, light scattering, NMR, and ESR experiments provide information on $C_2^s(t)$. The linear regimes in the curve reveal the emergence of the power law

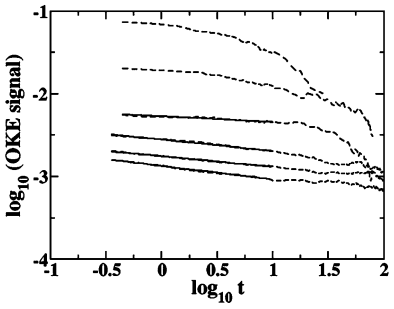

Figure 3. Time dependence of the OKE signal, which is proportional to the negative of the time derivative of the collective second-rank orientational time correlation function $C_2^c(t)$, in a log−log plot for a 500-particle model liquid crystalline system GB(3, 5, 2, 1) across the I−N transition at several temperatures. From top to bottom, the temperature, *T*, gradually drops: $T = 2.008$, 1.499, 1.396, 1.310, 1.192, and 1.102. Throughout this article, unless otherwise specified, the negative of the time derivative of the collective second-rank orientational time correlation function obtained computationally is labeled as the OKE signal for brevity. The continuous lines are the linear fits to the data, showing the power law decay regimes (data from ref 48).

decay at short to intermediate times near the I−N phase boundary.[48] As the system transits across the I−N phase boundary from the isotropic side, two power law decay regimes, separated by a plateau, appear, giving rise to a step-like feature.[36] In order to set a direct link with experimental results, we show in Figure 3 the temporal behavior of the negative of the time derivative of the collective second-rank OTCF, $C_2^c(t)$, that provides a measure of the OKE signal derived from this system. The collective second-rank OTCF is defined by

$$C_2^c(t) = \frac{<\sum_i \sum_j P_2(\hat{\mathbf{e}}_i(t)\cdot\hat{\mathbf{e}}_j(0))>}{<\sum_i \sum_j P_2(\hat{\mathbf{e}}_i(0)\cdot\hat{\mathbf{e}}_j(0))>} \qquad (3)$$

The power law regime is evident in the decay of the OKE signal over the short-to-intermediate time window as the I−N transition is approached upon cooling. The short-to-intermediate time power law decay persists in the nematic phase. In experiments, although the exponent of this power law was found to be independent[16] of temperature on the isotropic side of the I−N transition, it was found to depend[26] on temperature in the nematic phase. In our simulations, however, the temperature dependence of the power law exponent is rather weak. The single-particle and collective orientational dynamics in calamitic liquid crystals have been investigated further in recent computational studies on either side of the I−N phase boundary.[54,55]

In the quest for a universal feature in the short-to-intermediate time orientational dynamics of thermotropic liquid crystals across the I−N transition, we investigated a model discotic system.[36] As a representative discotic system, we considered a system of *oblate* ellipsoids of revolution interacting with each other via a modified form of the GB pair potential, GBDII, which was suggested for disclike molecules by Bates and Luckhurst.[56] The parametrization, which we employed for the model discotic system, is $\kappa = 0.345$, $\kappa' = 0.2$, $\mu = 1$, $\nu = 2$. Figure 4a and b shows the time evolution of the single-particle second-rank OTCF and the OKE signal derived from the discotic system at several temperatures along an isobar. Again, we observe the emergence of the power law decay regime in the isotropic phase near the I−N transition. The short-to-intermediate time power law decay thus seems to be a universal feature in the orientational relaxation of thermotropic liquid crystals near the I−N transition. We note that although a power law decay of the OKE signal has been recently observed experimentally in calamitic systems near the I−N phase boundary and in the nematic phase,[12−14,26] our prediction on the discotic systems stands to be tested in experiments.

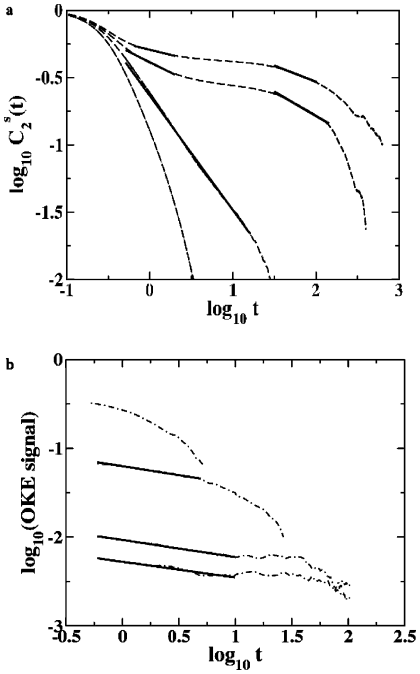

Figure 4. Orientational dynamics of the discotic system GBDII ($N = 500$) at several temperatures across the isotropic−nematic transition along the isobar at pressure $P = 25$. (a) Time evolution of the single-particle second-rank orientational time correlation function in a log−log plot. (b) The short-to-intermediate time decay of the OKE signal in a log−log plot. The dashed lines are the simulation data, and the continuous lines are the linear fits to the data, showing the power law decay regimes. The temperature, *T*, drops gradually from top to bottom in (b) and from bottom to top in (a). $T = 2.991$, 2.693, 2.646, and 2.594. In this case, the I−N transition is bracketed by 2.693 and 2.646 (data from ref 36).

When a different isobar was chosen at a lower pressure for the discotic system, a direct transition from the isotropic phase to the columnar phase was observed. In this case, decay of neither the single-particle second-rank OTCF nor the OKE signal showed any power law regime.[57] We note that the isotropic−columnar (I−C) transition is strongly first-order in nature, as reflected in the present case with a much larger change in the density corresponding to the I−C transition as compared to the I−N transition. The weakly first-order nature of the I−N transition thus appears to play a role in the origin of the short-to-intermediate time power law decay in orientation relaxation of thermotropic liquid crystals near the I−N phase boundary. However, the lack of power law decay in orientational relaxation of the discotic system in the isotropic phase near the I−C phase boundary is in contrast with the observation made in a very recent OHD-OKE experimental study.[27]

For the purpose of comparison, we now look into the orientational dynamics in the binary mixture that we studied. In Figure 5a and b, we show the time evolution of the single-particle second-rank OTCF and the OKE signal derived from the system in log−log plots at several temperatures down to $\sim T_c$. The slowdown in the dynamics is evident on approaching T_c upon cooling. A plateau is observed in the single-particle second-rank OTCF in the intermediate time scale. It is evident

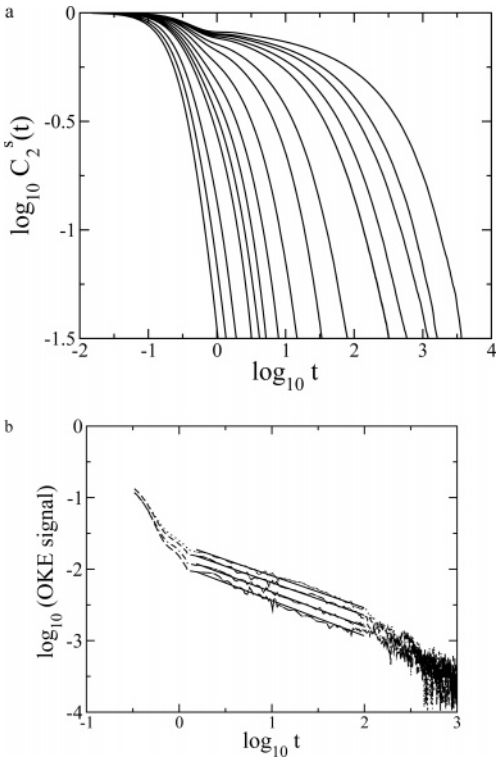

Figure 5. Orientational dynamics of the ellipsoids of revolution in the 50:50 binary mixture ($N = 256$) at several temperatures along the isochor at density $\rho = 0.8$. (a) Time evolution of the single-particle second-rank orientational time correlation function in a log−log plot. The temperature decreases from left to right ($4.997 \geq T \geq 0.498$). (b) Time dependence of the OKE signal in a log−log plot at temperatures $T = 0.574$, 0.550, 0.529, and 0.498. The continuous lines are linear fits showing the power law decay. The temperature decreases from top to bottom across the linear regime (data from ref 48).

in Figure 5b that a rather long power law decay regime ($\sim t^{-\alpha}$ with α falling between 0.450 and 0.495) is observed spanning over almost 2 decades of time in the intermediate time window. The exponent of this power law thus appears to be only weakly temperature-dependent, if at all. It may be recalled that recent OHD-OKE data for supercooled molecular liquids suggested a temperature-independent exponent for the intermediate power law.[16] However, the values of the exponent obtained here do not seem to agree with the experimentally observed value that is close to −1. The finite system size might have contributed to this lack of agreement.

2. Heterogeneous Dynamics. A large number of experimental and computer simulation studies have revealed signatures of heterogeneous dynamics in supercooled liquids.[58−60] Heterogeneous dynamics are now believed to underlie several features of complex dynamics observed in the supercooled regime.[58−60] Although the isotropic phase of a liquid crystalline system is macroscopically homogeneous, near the I−N transition, a local nematic-like order, which is attributed to the weakly first-order nature of the transition, persists over a length scale $\xi(T)$ that characterizes the so-called pseudonematic domains. The long-time exponential decay is ascribed to the randomization of these pseudonematic domains. The LdG theory predicts the correlation length, $\xi(T)$, to grow as the temperature, T, approaches T_{I-N} from above: $\xi(T) = \xi_0[T^*/(T - T^*)]^{1/2}$, where ξ_0 is a molecular length. It suggests that $\xi(T)$ eventually diverges at T^*, which falls just below T_{I-N} (typically, $T_{I-N} - T^* \sim 1$ K).[2] It is intuitive that the appearance of pseudonematic domains in the isotropic phase near T_{I-N} would result in heterogeneous dynamics. This led us to investigate heterogeneous dynamics

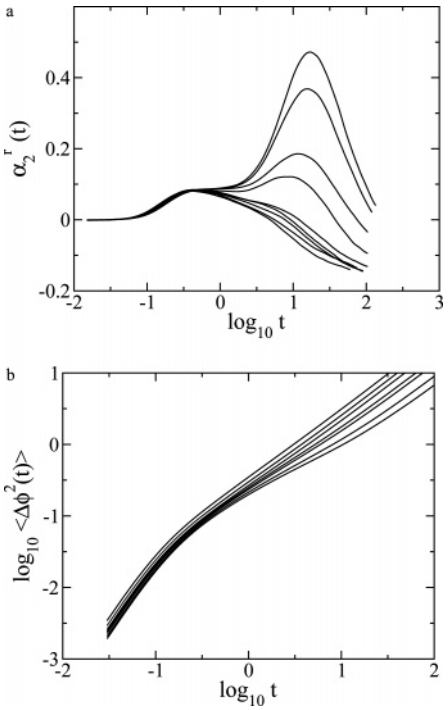

Figure 6. (a) Time dependence of the rotational non-Gaussian parameter $\alpha_2^r(t)$ in a semilog plot for the model liquid crystalline system GB(3, 5, 2, 1) ($N = 500$) at several temperatures $2.008 \geq T \geq 1.102$ across the I−N transition along the isochor at $\rho = 0.32$. The long-time peak gets stronger as the temperature gradually falls. (b) Time dependence of the mean square angular displacement for the same system at the same set of temperatures as mentioned above. The curves corresponding to two temperatures, where the system is in the isotropic phase, are removed for the clarity of the figure (data from ref 61).

near the I−N transition and across the supercooled regime and compare our results.[61] As a diagnostic of dynamical heterogeneity in ODOF, we defined the rotational non-Gaussian parameter[61] (NGP) as

$$\alpha_2^r(t) = \frac{\langle \Delta\Phi^4(t) \rangle}{2\langle \Delta\Phi^2(t) \rangle^2} - 1 \tag{5}$$

where

$$\langle \Delta\Phi^{2n}(t) \rangle = \frac{1}{N} \sum_{i=1}^{N} \langle |\Phi_i(t) - \Phi_i(0)|^{2n} \rangle \tag{5}$$

Here, Φ_i is the rotational analogue of the position $\mathbf{r}_i$ of the ith ellipsoid of revolution, the change of which is defined[62,63] by $\Delta\Phi_i(t) = \Delta\Phi_i(t) - \Delta\Phi_i(0) = \int_0^t dt' \omega_i(t')$, ω_i being the corresponding angular velocity. Figure 6a shows the time dependence of the rotational NGP $\alpha_2^r(t)$ for the model liquid crystalline system GB(3, 5, 2, 1) at several temperatures across the I−N transition. A bimodal feature appears with the growth of a second peak at longer times on approaching the I−N transition from the isotropic side. On crossing the I−N phase boundary, the long-time peak becomes the dominant one with a shoulder at shorter times. As the temperature is lowered, the onset of the growth of the long-time peak in the rotational NGP is accompanied by a signature of a subdiffusive regime in the temporal evolution of the mean square angular deviation as shown in Figure 6b. The time scale of the shoulder is also found to nearly coincide with that of the onset of the subdiffusive regime. The shoulder in the rotational NGP can therefore be ascribed to what may be called the rotational analogue of *rattling*

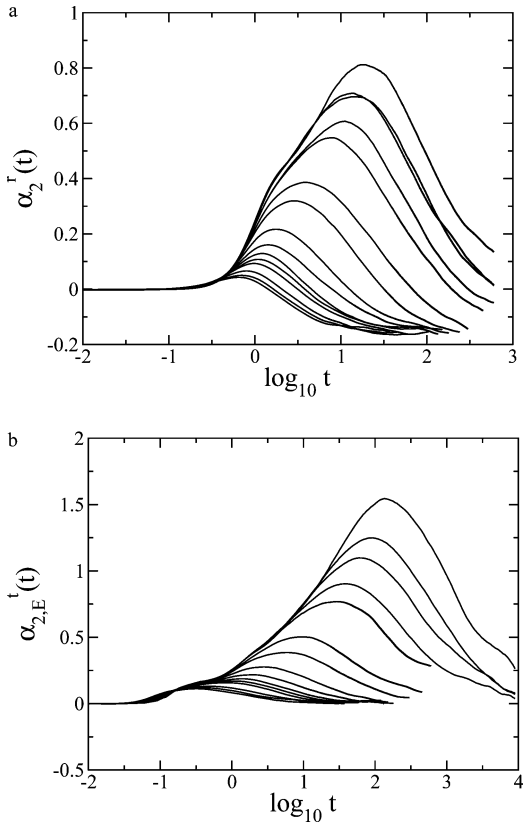

Figure 7. Time dependence of the non-Gaussian parameters in a semilog plot for the ellipsoid of revolution in the 50:50 binary mixture ($N = 256$) for all temperatures investigated. The temperature decreases gradually from bottom to top. (a) Time dependence of the rotational non-Gaussian parameter $\alpha_2^r(t)$ and (b) time dependence of the translational non-Gaussian parameter $\alpha_2^t(t)$ (data from ref 61).

within a cage. Subsequent to the shoulder, the dominant peak appears around a time t_{max}^r, which shifts rather slowly to higher values as the temperature falls. We note that t_{max}^r is comparable to the onset of the diffusive motion in ODOF. We further note that the time scale of the dominant peak also coincides with that of the plateau, which is observed in the time evolution of $C_2^s(t)$, as evident in Figure 2. It follows that the long-time peak appears with the growth of the pseudonematic domains that have random local directors and becomes pronounced as the orientational correlation grows.

In Figure 7, we show the time evolution of the rotational NGP as well as the translational NGP for the ellipsoid of revolution in the binary mixture. The latter is defined by

$$\alpha_2^t(t) = \frac{3\langle \Delta r^4(t)\rangle}{5\langle \Delta r^2(t)\rangle^2} - 1 \tag{6}$$

where

$$\langle \Delta r^{2n}(t)\rangle = \frac{1}{N}\sum_{i=1}^{N}\langle |r_i(t) - r_i(0)|^{2n}\rangle \tag{7}$$

It is evident in Figure 7a that the growth of the rotational NGP to its maximum value before it starts decaying is rather smooth at all the temperatures studied. The maximum is found to be reached on a time scale that characterizes the onset of the diffusive motion in ODOF. This time, t_{max}^r, gets lengthened with decreasing temperature. Although the short-time shoulder is not observed in the case of the rotational NGP, it appears in the time evolution of the translational NGP, as evident in Figure 7b. At high temperatures, starting from $\alpha_2^t(t = 0) = 0$, the translational NGP rises smoothly to a value α_{2max}^ton a time scale that characterizes the crossover from the ballistic to the diffusive motion in TDOF. It then starts falling off to reach the long time limit. As the temperature drops, a *shoulder* or a *steplike feature* appears between the initial rise and subsequent growth to its maximum value. The shoulder is found to appear as a subdiffusive regime sets in between the ballistic and diffusive motion. It is further observed that the shoulder in the translational NGP appears on a time scale that coincides with that of the second maximum of the velocity autocorrelation function (data not shown). The velocity autocorrelation function shows oscillatory character, particularly at low temperatures. The present analysis suggests that the shoulder at small times in the translational NGP can be attributed to what is known as the *rattling within a cage*, whereas the dominant peak appears on a time scale that characterizes the escape of a particle from the cage formed by its nearest neighbors. The absence of the steplike feature in the time dependence of the rotational NGP may be ascribed to the less pronounced freezing of the motion along ODOF.

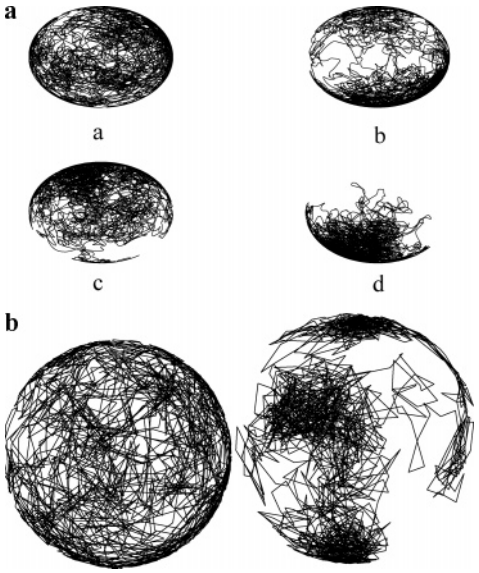

Figure 8. Typical single-particle trajectories of the unit orientational vector for an ellipsoid of revolution (a) in the model liquid crystalline system GB(3, 5, 2, 1) at four temperatures: (a) $T = 2.008$ (in the isotropic phase), (b) $T = 1.396$ (close to the I−N transition), (c) $T = 1.310$ (close to the I−N transition), and (d) $T = 1.192$ (in the nematic phase), and (b) in the model binary mixture at the highest (left) and the lowest (right) temperatures studied (data from ref 61).

3. A Microscopic View. In Figure 8, we present a microscopic view of single-particle trajectories in the orientational space. Such a view clearly demonstrates the onset of localization of the orientational motion around a preferred alignment as the I−N transition is approached upon cooling. The single-particle trajectories in Figure 8a provide the direct evidence of the rotational symmetry breaking on arrival at the nematic phase from the isotropic phase. It is to be noted that the interaction between the ellipsoids of revolution still retains the up−down symmetry. In Figure 8b, we display typical single-particle trajectories in the orientational space for ellipsoids of revolution in the binary mixture. Although the dynamics are ergodic at high temperatures, the signature of nonergodicity is evident at the lowest temperature studied. A comparison between Figure 8a and Figure 8b is revealing. For the model liquid crystalline

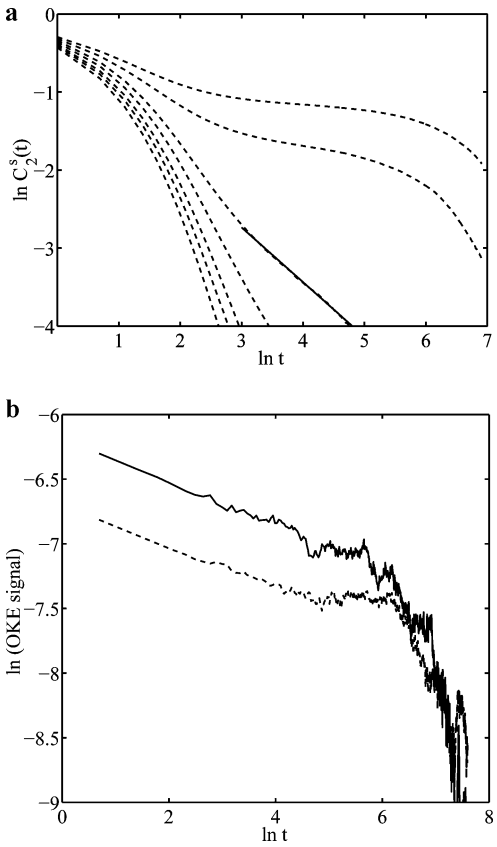

Figure 9. Time dependence of orientational relaxation in the model liquid crystalline system GB(3, 5, 2, 1) ($N = 576$) at several densities across the I−N transition along the isotherm at $T = 1$. (a) The single-particle second-rank orientational time correlation function in a log−log plot. From left to right, the density gradually increases from $\rho = 0.285$ to $\rho = 0.315$ in steps of 0.005. The continuous line is a fit to the power law regime. (b) The OKE signal, measured by the negative of the time derivative of the collective second-rank orientational time correlation function $C_2^c(t)$ in a log−log plot. The dashed line corresponds to $\rho = 0.31$, and the continuous line to $\rho = 0.315$ (data from ref 64).

system, the seemingly "nonergodic" behavior is driven by the rotational anisotropy that emerges near the I−N transition.[61]

4. Density Dependent Studies. Most of the computational studies described here were carried out by varying the temperature at a constant density across the I−N phase boundary. When the density is varied along an isotherm, the I−N phase boundary in the present system is known to be relatively sharp, and one is left with a rather narrow window to observe the pretransition effects. Nevertheless, a similar evolution of the orientational relaxation pattern, for both the single-particle and collective orientation dynamics, was observed when the density was varied as a control parameter at a constant temperature across the I−N transition.[55,64] The emergence of the power law decay at short to intermediate times near the I−N phase boundary is evident in Figure 9a and Figure 9b.

5. Fragility of Calamitic Liquid Crystals. The remarkable similarity in the spectrum of relaxation behavior exhibited by calamitic liquid crystals across the I−N phase boundary and supercooled liquids calls for a quantitative estimation of the extent of glassy dynamics in the former. For glass forming liquids, the plot, which displays the shear viscosity (or the structural relaxation time, the inverse diffusivity, etc.) in a logarithmic scale as a function of the inverse temperature scaled by T_g,[65−67] provides the basis of a quantitative measurement in terms of the fragility index, *m*. In a similar spirit, the single-

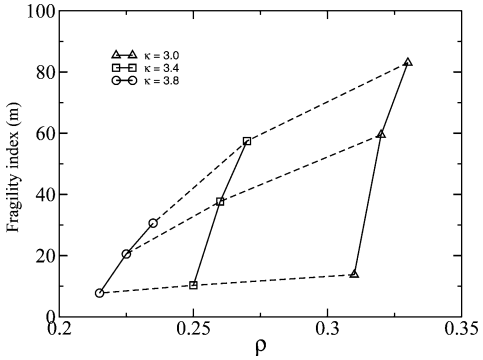

Figure 10. The fragility index, *m*, as a function of density for different aspect ratios of model calamitic systems. The systems considered are GB(3, 5, 2, 1), GB(3.4, 5, 2, 1), and GB(3.8, 5, 2, 1). In each case, $N = 500$ (data from ref 68).

particle second-rank orientational correlation time $\tau_2^s(T)$ was plotted (not shown here) in the logarithmic scale as a function of the inverse temperature along three isochors for three Gay−Berne systems GB(κ, 5, 2, 1), which differed only in the choice of the aspect ratio.[68] In such a plot, the temperature was scaled by the I−N transition temperature T_{I-N}, which was taken as the temperature at which the average orientational order parameter of the system was 0.35. An estimate of $\tau_2^s(T)$ was obtained as the time taken for $C_2^s(t)$ to decay by 90%, that is, $C_2^s(t = \tau_2^s) = 0.1$. For all the three systems, two distinct features are found to be common: (i) in the isotropic phase far away from the I−N transition, the orientational correlation time exhibits Arrhenius temperature dependence, that is, $\tau_2^s(T) = \tau_0 \exp[E_0/(k_B T)]$, where the activation energy E_0 and the infinite temperature relaxation time τ_0 are independent of temperature; (ii) in the isotropic phase near the I−N transition, the temperature dependence of $\tau_2^s(T)$ shows marked deviation from Arrhenius behavior and can be well described by the Vogel−Fulcher−Tammann (VFT) equation, $\tau_2^s(T) = \tau_{VFT} \exp[B/(T - T_{VFT})]$, where τ_{VFT}, B, and T_{VFT} are constants, independent of temperature. Again, these features bear remarkable similarity with those observed for fragile glass-forming liquid. A non-Arrhenius temperature behavior is taken to be the signature of fragile liquids. For fragile liquids, the temperature dependence of the shear viscosity follows Arrhenius behavior far above T_g and can be fitted to the VFT functional form in the deeply supercooled regime near T_g.[65−67] In the same spirit that offers a quantitative estimation of the fragile behavior of supercooled liquids, we defined[68] the fragility index of a liquid crystalline system as

$$m = \left.\frac{\mathrm{d} \log \tau_2^s}{\mathrm{d}(T_{I-N}/T)}\right|_{T = T_{I-N}} \quad (8)$$

Figure 10 shows the density dependence of the fragility index for the three systems with different aspect ratios. For a given aspect ratio, the fragility index increases with increasing density. The numerical values of the fragility index *m* are found to be comparable to those of supercooled liquids. The change in the fragility index for a given density difference ($\Delta\rho$) increases with the decrease in the aspect ratio.

VI. Energy Landscapes of Calamitic Liquid Crystals. A useful framework for interpreting the thermodynamic and dynamic properties of condensed phase is provided by the energy landscape[24] picture, which, in particular, has been extensively used for elucidation of dynamics of supercooled liquids.[20,22,23] By energy landscape, what is meant is the

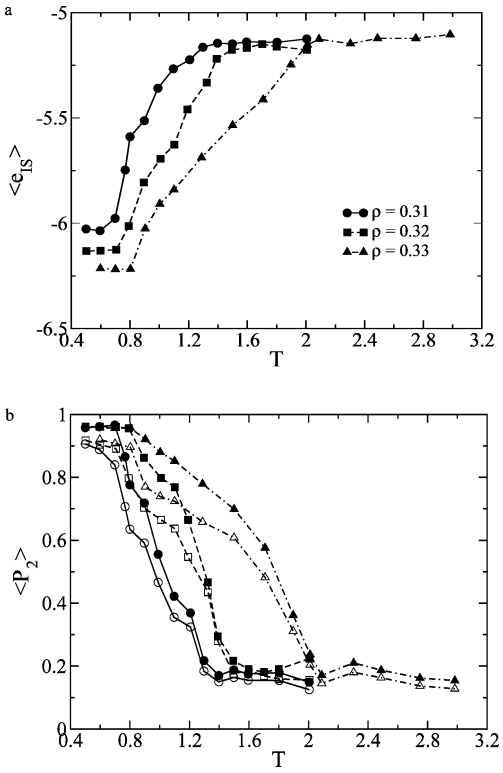

Figure 11. The potential energy landscape explored by the model calamitic system GB(3, 5, 2, 1) ($N = 256$) as the system passes through different mesophases upon cooling. (a) Temperature dependence of the average inherent structure energy per particle, $<e_{IS}>$, along three isochors at densities $\rho = 0.31$, 0.32, 0.33. (b) Evolution of the average orientational order parameter $<P_2>$ with temperature for both the inherent structures (filled) and the corresponding prequenched configurations (opaque) (data from ref 69).

hyperspace generated upon representing the potential energy of an N-body system as a function of all configurational coordinates, $\{q_i\}$. For the simplest case of an N-particle atomic system, which is devoid of orientational and vibrational degrees of freedom, the energy landscape is $3N + 1$ dimensional hyperspace. The inception of the energy landscape picture was the classic contribution by Goldstein in 1969 when he formulated what he called "a potential energy barrier picture" of flow and relaxation in viscous liquids.[20] Subsequently, Stillinger and co-workers, building upon the foundation laid down by Goldstein, proposed a computational approach to develop the energy landscape picture.[21] In this approach, the potential energy surface is partitioned into a large number of *basins*, each defined as the set of points in the multidimensional configuration space such that a local minimization of the potential energy maps each of these points to the same local minimum. The configuration corresponding to a minimum is known as an *inherent structure* (IS).[21]

Figure 11a displays the average inherent structure energy per particle as the change in the temperature drives the system GB(3, 5, 2, 1) across mesophases along three different isochors. The isochors were so chosen that the range of the nematic phase along these isochors varied considerably.[69] Apart from the isotropic phase, this system is known to exhibit the nematic and smectic-B phases, but no smectic-A phase.[45] Although the smectic-A phase has liquidlike order in the layers perpendicular to the director, there exists hexagonal order in these layers in the smectic-B phase. Figure 11b shows the concomitant evolution of the average orientational order parameter $<P_2>$ for both the inherent structures and the corresponding prequenched

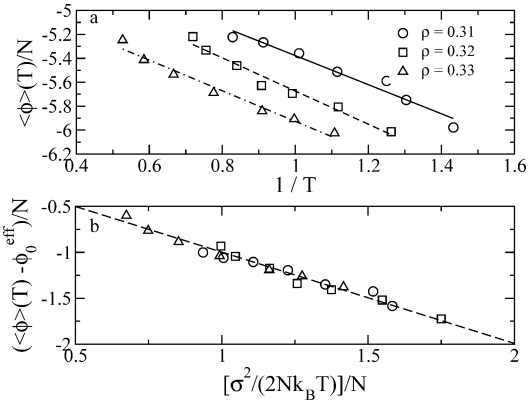

Figure 12. Validity of the Gaussian model for the number density of the inherent structure energy for the model calamitic system GB(3, 5, 2, 1) ($N = 256$). (a) Average inherent structure (IS) energy per particle as a function of the inverse temperature at different densities. The continuous line, dashed line, and dotted−dashed lines are the linear fits to the data at densities $\rho = 0.31$, 0.32, and 0.33, respectively. (b) Displaced average IS energy per particle versus a scaled inverse temperature along the same three isochors. If the Gaussian model for the number density of the IS energy is validated, a collapse of the data for all densities is expected onto the straight line with negative unit slope, which is drawn. The data are shown over the temperature regimes in which the average IS energy is on a decline (data from ref 68).

configurations. It is evident that the average inherent structure energy remains fairly insensitive to temperature in the isotropic phase before it starts undergoing a steady fall below a certain temperature that corresponds to the onset of growth of the orientational order. As the orientational order grows through the nematic phase, the system continues to explore increasingly deeper potential energy minima. The transition from the nematic phase to the smectic phase in the parent system, signaled by the appearance of a one-dimensional density wave in the parallel radial distribution function[45] $g_{||}(r_{||})$ computed from prequenched configurations, results again in an average inherent structure energy that is roughly independent of temperature.

The fall in the average IS energy is consistent with a Gaussian form for the number density of inherent structure energy, e_{IS}, that predicts a linear variation of $<e_{IS}>$ with the inverse temperature: $<e_{IS}(T)> = e_0^{eff} - \sigma^2/(2Nk_BT)$, where e_0^{eff} and σ are parameters independent of temperature. Figure 12 a demonstrates that the prediction holds good over the temperature range where $<e_{IS}>$ is on a decline along all the three isochors studied. It then follows that a plot of $<e_{IS}(T)> - e_0^{eff}$ versus $\sigma^2/(2Nk_BT)$ would result in a collapse of the $<e_{IS}(T)>$ data for all densities onto a straight line with negative unit slope. This is, indeed, found to be true, as shown in Figure 12b, implying the validity of the Gaussian model in this case over a temperature range where the orientational order continues to grow upon cooling.[68]

The manner in which the present system[69] samples its potential energy landscape is remarkably similar to what was observed for a model system of glass-forming liquids, even though the latter avoided a phase transition.[23,70] In an appealing landscape study of a binary Lennard-Jones mixture, Sastry et al. revealed that a crossover temperature, below which the average depth of the potential energy minima explored by the system grows, marks the onset of the breakdown of Arrhenius behavior in the temperature dependence of the structural relaxation time.[23] In search of a correlation between the exploration of the underlying energy landscape by the system and its dynamics, we show the Arrhenius representation of the temperature-dependent data of the single-particle orientational

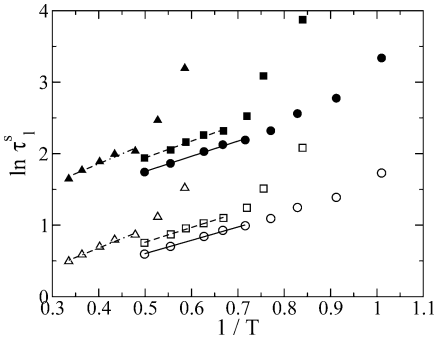

Figure 13. Breakdown of Arrhenius behavior in orientational dynamics of the model calamitic system GB(3, 5, 2, 1) ($N = 256$). The inverse temperature dependence of the single-particle orientational relaxation times, τ_l^s, $l = 1$ (filled) and $l = 2$ (opaque), in the logarithmic scale. The straight lines are Arrhenius fits to the subsets of data points, each set corresponding to an isochor: $\rho = 0.31$ (circle), $\rho = 0.32$ (square), and $\rho = 0.33$ (triangle) (data from ref 69).

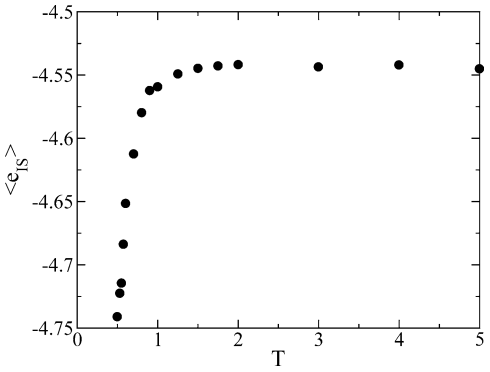

Figure 14. Average inherent structure energy per particle, $<e_{IS}>$, as a function of temperature for the 50:50 binary mixture of the Lennard-Jones spheres and the Gay−Berne ellipsoids of revolution ($N = 256$) over the whole temperature range studied (data from ref 71).

relaxation times in Figure 13. In this case,[69] a measure of the relaxation time $\tau_l^s(T)$ was taken as the time when $\tau_l^s(t) = e^{-1}$, as in ref (23). Figure 13 illustrates the dramatic slowdown of orientational dynamics with decreasing temperature near the I−N transition for $l = 1,2$. It follows that in the isotropic phase far from the I−N transition region $\tau_l^s(T)$ exhibits Arrhenius behavior, that is, $\tau_l^s(T) = \tau_{0,l} \exp[E_l/(k_B T)]$, where the activation energy E_0 and the infinite temperature relaxation time $\tau_{0,l}$ are independent of temperature. We find that Arrhenius behavior breaks down near the I−N transition, and this breakdown occurs at a temperature that marks the onset of growth of the average depth of the potential energy minima explored by the system.[69] For the binary mixture we investigated, the average depth of the potential energy minima sampled by the system was also found to grow with decreasing temperature below a certain onset temperature, as shown in Figure 14.[71] In this case, the low-temperature plateau, which is missing, unlike in ref 23, seems to be beyond the temperature range of investigation. The onset temperature was found to mark the breakdown of the Debye model of rotational diffusion, which ceases to be valid at lower temperatures.[71] The Debye model of rotational diffusion was also demonstrated to break down for calamitic liquid crystals near the I−N phase boundary due to the growth of the orientational correlation.[72]

It is to be noted that while the emergence of the power law decay near the I−N transition is coincident with growing orientational correlation, the system explores deeper potential energy minima as the orientational order parameter grows through the nematic phase upon cooling. This suggests a plausible connection between the power law relaxation and the exploration of the underlying energy landscape. In fact, the exponent of the intermediate power law observed in the OKE experiments in the nematic phase has been found to be linearly dependent on the orientational order parameter.[26,27] It would therefore be instructive to explore the correspondence between the power law relaxation and the features of the energy landscape in further details.

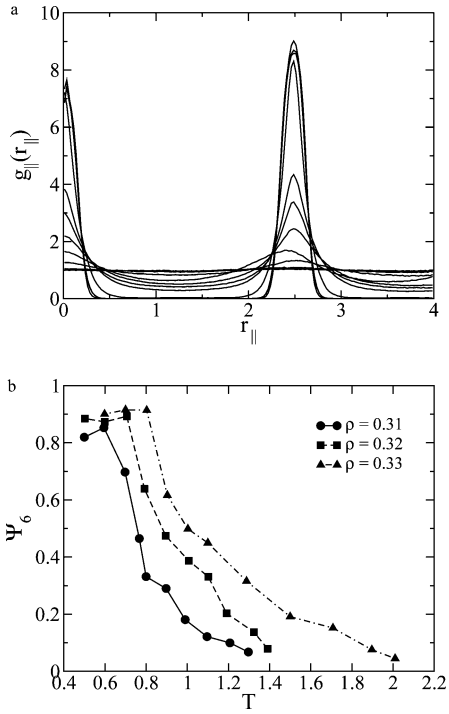

Figure 15. Characterization of the inherent structures for the model calamitic system GB(3, 5, 2, 1) ($N = 256$). (a) Parallel radial distribution function $g_{||}(r_{||})$ for the inherent structures at all 15 temperatures considered along the isochor at density $\rho = 0.32$. Note that the curves for the highest five temperatures are nearly superposed on each other. For others, the amplitude of the peaks gradually increases as temperature drops. (b) Evolution of the 6-fold bond orientational order parameter Ψ_6 for the inherent structures with temperature at three densities (data from ref 69).

VII. Structural Features of Inherent Structures

The structural features of the inherent structures yielded important information on the interplay between the orientational and translational order in the calamitic mesophases.[69] It follows from Figure 10b that quenching results in more enhanced orientational order for inherent structures than the corresponding prequenched configurations. We now examine how the inherent structures evolve as revealed by the pair distribution functions that were obtained by averaging over the quenched configurations. An analysis through parallel radial distribution function $g_{||}(r_{||})$, which depends only on $r_{||} = \mathbf{r}\cdot\hat{\mathbf{n}}$, the pair separation, r, parallel to the director, $\hat{\mathbf{n}}$, reveals a remarkable feature, as illustrated in Figure 15a. The onset of growth of the orientational order in the vicinity of the I−N transition induces a translational order in layers in the underlying quenched configurations. Such smecticlike layering is characterized by the one-dimensional density wave along the layer normal appearing in $g_{||}(r_{||})$. The amplitude of the density wave in inherent structures grows stronger as the orientational order increases through the nematic phase of the parent system and tends to attain saturation as the smectic phase sets in. An exploration of the parameter space

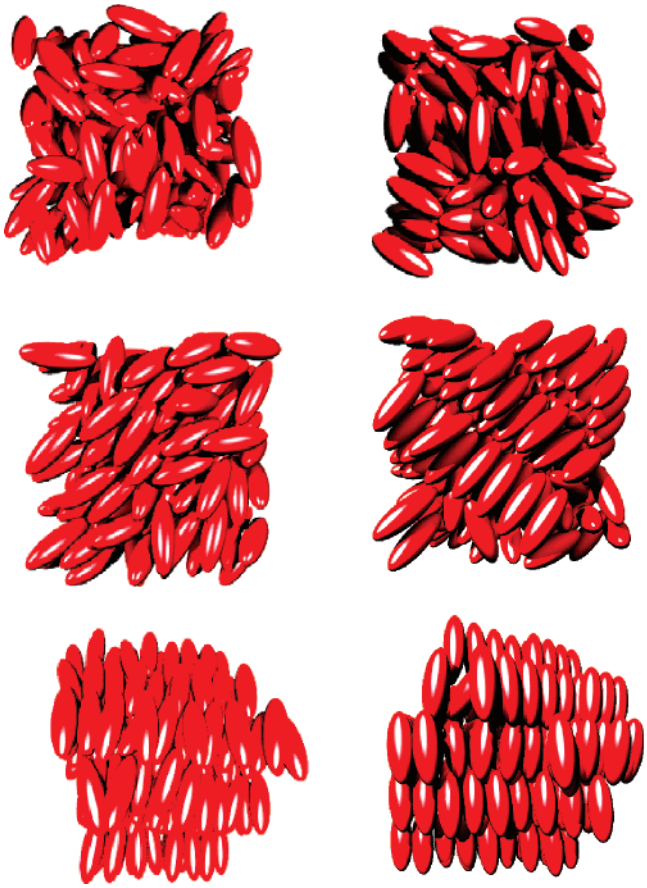

Figure 16. Typical snapshots of the model calamitic system GB(3, 5, 2, 1) in various phases obtained from molecular dynamics trajectories (left column) and the inherent structures (right column): isotropic phase, nematic phase, and smectic phase (from top to bottom).

suggested that the inherent structures never sustain orientational order alone, even when the parent phase is nematic, if the nematic phase is sandwiched between the high-temperature isotropic phase and the low-temperature smectic phase.[69] Thus, the stability of the nematic phase appears to be due to a subtle balance between the energy and the entropy, the former favoring it over the isotropic phase and the latter over the smectic phase. In Figure 16, we show typical snapshots of the parent system in various phases obtained from molecular dynamics trajectories and the inherent structures. The induction of translational order in the inherent structures when the parent phase is nematic is evident.

In the evolution of the perpendicular radial distribution function $g_\perp(r_\perp)$ for the inherent structures, the gradual enhancement of order is evident, and the peaks that follow the dominant one are found to be split.[69] This is typical of quenched configurations and, hence, is inconclusive for the inherent structures to be categorized as either smectic-A or smectic-B. We therefore computed the 6-fold bond orientational order parameter,[73] Ψ_6, for the inherent structures to characterize the smectic phase further on the basis of hexagonal symmetry. As shown in Figure 15b, we find that as the system passes through the nematic phase upon cooling, concomitant with the growth of the translational order in the inherent structures, Ψ_6 also grows until it attains saturation with the advent of the smectic-B phase in the system. It seems therefore reasonable to conclude that as the system makes a passage across the nematic phase from the high-temperature isotropic to the low-temperature smectic-B phase, the underlying potential energy minima evolve from the isotropic to the smectic-B phase through the smectic-A phase with no signature of the nematic phase.

VIII. Conclusion

It is well-known that the isotropic phase of liquid crystals exhibits an exponential decay of the orientational time correlation function at long times near the isotropic−nematic phase boundary. The time constant of this decay is known as the LdG time, and this constant grows rapidly as the I−N phase transition is approached upon cooling. In the past, slow dynamics were investigated in the nematic phase where fluctuations of the director were studied at length and discussed theoretically in several well-known studies. However, all these earlier studies were restricted to times longer than hundreds of nanoseconds, mostly in the microsecond to millisecond time range. Recent time domain OKE experiments, which required the advancement of optical and spectroscopic techniques to attain the current level of sophistication, could investigate a much wider time window ranging from subpicoseconds to tens of microseconds. The emergence of such rich dynamical behavior in the short-to-intermediate time window (smaller than nanoseconds) is really surprising.

In this article, we have focused largely on the orientational dynamics of calamitic liquid crystals across the I−N transition in computer simulation studies of model systems. We have compared the results of calamitic liquid crystals with those of supercooled liquids. The experimentally observed short-to-intermediate time power law decay of the optical Kerr effect signal could be captured in our simulation studies of both systems. Additionally, a number of dynamical features, which are very similar to those of glassy dynamics, are on display for calamitic liquid crystals across the I−N phase boundary despite the difference in physical origin. These include two-step decay of the single-particle second- rank orientational time correlation function, subdiffusive regime in rotational motion, heterogeneous rotational dynamics, and the breakdown of the Debye model of rotational diffusion. A quantitative estimate of glassy dynamics of calamitic liquid crystals near the I−N phase boundary is attempted in terms of a "fragility index", which is found to have values comparable to those of glass-forming liquids. The similarity between calamitic liquid crystals and glass-forming liquids in the exploration of the underlying potential energy landscape is startling, even though the latter avoided a phase transition.[23] The correspondence of the breakdown of Arrhenius behavior of the temperature-dependent relaxation times with the exploration of deeper potential energy minima in both classes of soft matter systems is also noteworthy. The striking resemblance might imply a unique underlying landscape mechanism for slow dynamics in soft condensed matter. Moreover, our finding that the nematic phase in certain cases has no underlying inherent structures of its own kind may very well indicate a role of the smectic fluctuations in slow dynamics of calamitic liquid crystals near the I−N phase boundary and especially in the nematic phase. It is to be recognized that although recent OKE experiments have suggested similar relaxation behavior in the isotropic phase of calamitic liquid crystals near the I−N phase boundary and in supercooled molecular liquids, our computational studies reveal analogous features also beyond the I−N phase boundary into the nematic phase. In search of a probable unified description of dynamics of soft condensed matter systems, the present line of research is worth further pursuance.

Acknowledgment. We thank Professor Michael D. Fayer, Dr. Prasanth Jose, Suman Chakrabarty, and Biman Jana for

collaboration and helpful discussions. We also thank Dr. David J. Wales for many stimulating discussions and Szilard Fejer for assistance in preparing some of the graphics. This research was supported in part by grants from DST and CSIR, India and a Research Fellowship to D.C. by UGC, India. D.C. acknowledges the Marie Curie Incoming International Research Fellowship within the 6th European Community Framework Program.

References and Notes

(1) Chaikin, P. M.; Lubensky, T. C. *Principles of Condensed Matter Physics*; Cambridge University Press: Cambridge, 1998.
(2) de Gennes, P. G.; Prost, J. *The Physics of Liquid Crystals*; Clarendon Press: Oxford, 1993.
(3) Chandrasekhar, S. *Liquid Crystals*; Cambridge University Press: Cambridge, 1992.
(4) Roie, B. V.; Leys, J.; Denolf, K.; Glorieux, C.; Pitsi, G.; Thoen, J. *Phys. Rev. E: Stat. Phys., Plasmas, Fluids, Relat. Interdiscip. Top.* **2005**, *72*, 041702.
(5) Litster, J. D.; Stinson, III, T. W. *J. Appl. Phys.* **1970**, *41*, 1996.
(6) Prost, J.; Lalanne, J. R. *Phys. Rev. A: At., Mol., Opt. Phys.* **1973**, *8*, 2090.
(7) Hanson, E. G.; Shen, Y. R.; Wong, G. K. L. *Phys. Rev. A: At., Mol., Opt. Phys.* **1976**, *14*, 1281.
(8) Fillippini, J. C.; Poggi, Y. *Phys. Lett.* **1978**, *65A*, 30.
(9) Stankus, J. J.; Torre, R.; Marshall, C. D.; Greenfield, S. R.; Sengupta, A.; Tokmakoff, A.; Fayer, M. D. *Chem. Phys. Lett.* **1992**, *194*, 213.
(10) Stankus, J. J.; Torre, R.; Fayer, M. D. *J. Phys. Chem.* **1993**, *97*, 9478.
(11) Torre, R.; Tempestini, F.; Bartolini, Righini, R. *Philos. Mag. B* **1998**, *77*, 645.
(12) Gottke, S. D.; Brace, D. D.; Cang, H.; Bagchi, B.; Fayer, M. D. *J. Chem. Phys.* **2002**, *116*, 360.
(13) Gottke, S. D.; Cang, H.; Bagchi, B; Fayer, M. D. *J. Chem. Phys.* **2002**, *116*, 6339.
(14) Cang, H.; Li, J.; Fayer, M. D. *Chem. Phys. Lett.* **2002**, *366*, 82.
(15) Drozd-Rzoska, A.; Rzoska, S. J. *Phys. Rev. E: Stat. Phys., Plasmas, Fluids, Relat. Interdiscip. Top.* **2002**, *65*, 041071.
(16) Cang, H.; Li, J.; Novikov, V. N.; Fayer, M. D. *J. Chem. Phys.* **2003**, *118*, 9303.
(17) Angell, C. A.; Ngai, K. L.; McKenna, G. B.; McMillan, P. F.; Martin, S. W. *J. Appl. Phys.* **2000**, *88*, 3113.
(18) Debenedetti, P. G.; Stillinger, F. H. *Nature* **2001**, *410*, 259.
(19) Pasini, P., Zannoni, C. Eds.; *Advances in the Computer Simulations of Liquid Crystals*; Kluwer Academic Publishers: Dordrecht, 2000.
(20) Goldstein, M. *J. Chem. Phys.* **1968**, *51*, 3728.
(21) Stillinger, F. H.; Weber, T. A. *Phys. Rev. A: At., Mol., Opt. Phys.* **1983**, *28*, 2408.
(22) Heuer, A. *Phys. Rev. Lett.* **1997**, *78*, 4051.
(23) Sastry, S.; Debenedetti, P. G.; Stillinger, F. H. *Nature* **1998**, *393*, 554.
(24) Wales, D. J. *Energy Landscapes*; Cambridge University Press: Cambridge, 2003.
(25) Torre, R.; Bartolini, P.; Pick, R. M. *Phys. Rev. E: Stat. Phys., Plasmas, Fluids, Relat. Interdiscip. Top.* **1998**, *57*, 1912.
(26) Li, J.; Wang, I.; Fayer, M. D. *J. Phys. Chem. B* **2005**, *109*, 6514.
(27) Li, J.; Wang, I; Fayer, M. D.; *J. Chem. Phys.* **2006**, *124*, 044906.
(28) Cang, H.; Novikov, V. N.; Fayer, M. D. *Phys. Rev. Lett.* **2003**, *90*, 197401.
(29) Cang, H.; Novikov, V. N.; Fayer, M. D. *J. Chem. Phys.* **2003**, *118*, 2800.
(30) Lunkenheimer, P.; Pimenov, A.; Loidl, A. *Phys. Rev. Lett.* **1997**, *78*, 2995.
(31) Sokolov, A. P.; Kisliuk, A.; Novikov, V. N.; Ngai, K. *Phys. Rev. B: Condens. Matter Mater. Phys.* **2001**, *63*, 172204.
(32) Ngai, K. L.; Habasaki, J.; Hiwatari, Y.; Léon, C. *J. Phys.: Condens. Matter.* **2003**, *15*, S1607.
(33) Bengtzelius, U.; Götze, W.; Sjolander, A. *J. Phys. C* **1984**, *17*, 5915.
(34) Götze, W.; Sperl, M. *Phys. Rev. Lett.* **2004**, *92*, 105701.
(35) Li, J.; Cang, H.; Andersen, H. C.; Fayer, M. D. *J. Chem. Phys.* **2006**, *124*, 014902.
(36) Chakrabarti, D.; Jose, P. P.; Chakrabarty, S.; Bagchi, B. *Phys. Rev. Lett.* **2005**, *95*, 197801.
(37) Chaudhury, S.; Cherayil, B. J. *J. Chem. Phys.* **2006**, *125*, 184505.
(38) Habasaki, J.; Ngai, K. L. *J. Non-Cryst. Solids* **2006**, *352*, 5170.
(39) Gilroy, K. S.; Phillips. W. A. *Philos. Mag. B* **1981**, *43*, 735.
(40) Novikov. V. N. *Phys. Rev. B: Condens. Matter Mater. Phys.* **1997**, *55*, R14685.
(41) Zannoni, C. *J. Mater. Chem.* **2001**, *11*, 2637.
(42) Allen, M. P.; Evans, G. T.; Frenkel, D.; Mulder, B. M. *Adv. Chem. Phys.* **1993**, *86*, 1.
(43) Andersen, H. C.; Chandler, D.; Weeks, J. D. *Adv. Chem. Phys.* **1976**, *34*, 105.
(44) Gay, J. G.; Berne, B. J. *J. Chem. Phys.* **1981**, *74*, 3316.
(45) Brown, J. T.; Allen, M. P.; del Rìo, E. M.; de Miguel, E. *Phys. Rev. E: Stat. Phys., Plasmas, Fluids, Relat. Interdiscip. Top.* **1998**, *57*, 6685.
(46) de Miguel, E.; Vega, C. *J. Chem. Phys.* **2002**, *117*, 6313.
(47) Bates, M. A.; Luckhurst, G. R. *J. Chem. Phys.* **1999**, *110*, 7087.
(48) Chakrabarti, D.; Bagchi, B. *J. Chem. Phys.* **2007**, *126*, 204906.
(49) Kob, W. *J. Phys.: Condens. Matter* **1999**, *11*, R85.
(50) Andersen, H. C. *Proc. Natl. Acad. Sci. U.S.A.* **2005**, *102*, 6686.
(51) Cleaver, D. J.; Care, C. M.; Allen, M. P.; Neal, M. P. *Phys. Rev. E: Stat. Phys., Plasmas, Fluids, Relat. Interdiscip. Top.* **1996**, *54*, 559.
(52) Antypov, D.; Cleaver, D. J. *J. Chem. Phys.* **2004**, *120*, 10307.
(53) Zannoni, C. In *Advances in the Computer Simulations of Liquid Crystals*; Pasini, P., Zannoni, C., Eds.; Kluwer Academic Publishers: Dordrecht, 2000.
(54) Bertolini, D.; Cinacchi, G.; Gaetani, L. D.; Tani, A. *J. Phys. Chem. B* **2005**, *109*, 24480.
(55) Jose, P. P.; Bagchi, B. *J. Chem. Phys.* **2006**, *125*, 184901.
(56) Bates, M. A.; Luckhurst, G. R. *J. Chem. Phys.* **1996**, *104*, 6696.
(57) Chakrabarti, D.; Jana, B.; Bagchi, B. *Phys. Rev. E: Stat. Phys., Plasmas, Fluids, Relat. Interdiscip. Top.* **2007**, *75*, 061703.
(58) Sillescu, H. *J. Non-Cryst. Solids* **1999**, *243*, 81.
(59) Ediger, M. D. *Annu. Rev. Phys. Chem.* **2000**, *51*, 99.
(60) Richert, R. *J. Phys.: Condens. Matter* **2002**, *14*, R703.
(61) Jose, P. P.; Chakrabarti, D.; Bagchi; B. *Phys. Rev. E: Stat. Phys., Plasmas, Fluids, Relat. Interdiscip. Top.* **2005**, *71*, 030701(R) .
(62) Kämmerer, S.; Kob, W.; Schilling, R. *Phys. Rev. E: Stat. Phys., Plasmas, Fluids, Relat. Interdiscip. Top.* **1997**, *56*, 5450.
(63) De Michele, C.; Leporini, D. *Phys. Rev. E: Stat. Phys., Plasmas, Fluids, Relat. Interdiscip. Top.* **2001**, *63*, 036702.
(64) Jose, P. P.; Bagchi, B. *J. Chem. Phys.* **2004**, *120*, 11256.
(65) Angell, C. A. *J. Phys. Chem. Solids* **1988**, *49*, 863.
(66) Angell, C. A. *J. Non-Cryst. Solids* **1991**, *131*−*133*, 13.
(67) Böhmer, R.; Ngai, K. L.; Angell, C. A.; Plazek, D. J. *J. Chem. Phys.* **1993**, *99*, 4201.
(68) Jana, B.; Chakrabarti, D.; Bagchi, B. *Phys. Rev. E: Stat. Phys., Plasmas, Fluids, Relat. Interdiscip. Top.* **2007**, *76*, 011712.
(69) Chakrabarti, D.; Bagchi. B. *Proc. Natl. Acad. Sci. U.S.A.* **2006**, *103*, 7217.
(70) Sastry, S. *Nature* **2001**, *409*, 164.
(71) Chakrabarti, D.; Bagchi, B. *Phys. Rev. Lett.* **2006**, *96*, 187101.
(72) Jose, P. P.; Chakrabarti, D.; Bagchi, B. *Phys. Rev. E: Stat. Phys., Plasmas, Fluids, Relat. Interdiscip. Top.* **2006**, *73*, 031705.
(73) Strandburg, K. J. Ed.; *Bond-Orientational Order in Condensed Matter Physics*; Springer-Verlag: New York, 1992.